Nonlinear Observer Design for Two-Phase Flow Heat Exchangers of Air Conditioning Systems

Tao Cheng, Xiang-Dong He, *Member*, *ASME* and H. Harry Asada, *Fellow*, *ASME*

Abstract— **This paper presents the design of a model-based nonlinear observer of an evaporator (a two-phase flow heat exchanger) for advanced dynamic control of air conditioning and refrigeration systems. A control-oriented, low-order model is derived for the evaporator. Based on sensor measurements of the evaporating temperature, the nonlinear observer can be used to estimate the heat transfer rate and the length of two-phase section that can not be measured directly. The convergence of the observer is proved using contraction theory. The simulation results and experimental testing also demonstrate the convergence. In air conditioning and refrigeration applications, the nonlinear observer can be utilized to synthesize feedback linearization nonlinear control and provide accurate refrigerant charge inventory estimation and optimization.**

I. Introduction

Two-phase flow heat exchangers have been widely used in air conditioning and refrigeration systems for residential, commercial, and industrial applications. Modeling, estimation, and control of two-phase flow heat exchangers have been active research subjects for years in attempts to imrove energy efficiency and system reliability. Most of these projects are concerned with the steady-state operation of such heat exchangers, despite the fact that steady-state conditions are almost never reached in the presence of dynamic interaction and varying environmental conditions. Modeling of dynamic behavior of a complicated and spatially distributed air conditioning system has been reported in several works [Chi and Didion, 1982], [MacArthur and Grald, 1989], [He, Liu and Asada, 1997], and [He and Asada, 2003]etc.

With increasing complexity of modern HVAC systems, controlling and optimizing the operation with guaranteed performance, stability and reliability becomes a challenging issue. In advanced control of HVAC systems, it is necessary to dynamically estimate some immeasurable variables based on available sensor measurements. For example, in the nonlinear feedback linearization [He and Asada, 2003], the heat transfer rate of evaporators must be estimated because no direct measurement is available. Dynamic estimation of heat transfer rate can also be used for adaptive control of room air temperature. To estimate the refrigerant charge inventory, it is necessary to know the two-phase section length of heat exchanger for an accurate estimate of refrigerant in the heat exchanger. Yet, this length of two-phase section is not directly measurable.

Despite many potential applications of heat exchanger observers, HVAC systems are nonlinear, hence, standard linear observers are not applicable. In this paper we will develop a nonlinear observer based on the contraction theory by [Lohmiller and Slotine, 1998]. In the following, a low-order model is developed for an evaporator. The model describes the dynamic relationship between the evaporating temperature and the compressor side mass flow rate that can be further related to compressor speed. The model also describes the dynamic relationship between the length of two-phase section of the evaporator and the expansion valve side mass flow rate that can be further related to expansion valve opening. The evaporator wall temperature is also treated as an independent state variable to improve the model accuracy. With this low-order model, a nonlinear observer can be designed to estimate heat transfer rate and the length of the two-phase section based on the sensor measurement of evaporating temperature. Contraction theory [Lohmiller and Slotine, 1998] is applied to guarantee the convergence with the proper selection of the observer gains.

This paper will be organized as follows. Section 2 will present a low-order model of the evaporator for the observer design. Section 3 will present a nonlinear observer design based on the evaporator model, and the analysis of convergence is carried out based on contraction theory. Simulation and experimental results will be discussed in Section 4. Section 5 will present an integrated control method combining nonlinear control and the observer design described in Section 3.

II. Dynamic Evaporator Model for Observer Design

This section describes a low-order evaporator model that will be used for the design of an observer. It is assumed that (1) the heat exchanger is a long, thin, horizontal tube; (2) the refrigerant flowing through the heat exchanger tube can be modeled as one-dimentional fluid flow; (3) axial heat conduction is negligible.

A diagram of a low-order evaporator model is illustrated in Fig. 1.

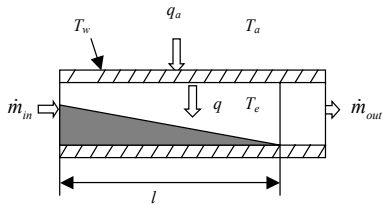

Fig.1.A diagram of a low-order evaporator model

$T_e(t)$ is the evaporating temperature, $l(t)$ is the length of the two-phase section. $T_w(t)$ is the wall temperature of the tube. T_a is the room air temperature. $\dot{m}_{in}$ and $\dot{m}_{out}$ are the inlet and outlet refrigerant mass flow rates, respectively. $q(t)$ is the heat transfer rate from the tube wall to the two-phase refrigerant. q_a is the heat transfer rate from the room to the tube wall. It is assumed that the two-phase section has invariant mean void fraction $\bar{\gamma}$ [Wedekind, Bhatt and Beck, 1978].

It can be assumed that the evaporator tube wall temperature along the two-phase section is spatially uniform. Then the energy balance equation of the tube wall is given by:

$$(c_p \rho A)_e \frac{dT_w}{dt} = \pi D_o \alpha_o (T_a - T_w) - \pi D_i \alpha_i (T_w - T_e) \qquad (1)$$

where c_p is the specific heat of the copper tube, ρ is the density of copper, A is the cross section area of the copper tube; D_o is the outer diameter, D_i is the inner diameter, α_o is the heat transfer coefficient between room air and the tube wall, and α_i is the heat transfer coefficient between refrigerant and the tube wall.

The first term on the right hand side of Eq. (1) represents the heat transfer rate per unit length from the room to the tube wall. The second term represents the heat transfer rate per unit length from the tube wall to the two-phase refrigerant.

Assuming the mean void fraction $\bar{\gamma}$ is invariant or changes very slowly compared to the state variables, the liquid mass balance equation in the two-phase section of the evaporator is

$$\rho_l (1-\bar{\gamma}) A \frac{dl(t)}{dt} = -\frac{q}{h_{\lg}} + \dot{m}_{in}(1-x_0) \qquad (2)$$

where ρ_l is the refrigerant saturated liquid density, q is the heat transfer rater between the tube wall and refrigerant in the two-phase section, x_0 is the inlet vapor quality, and $\dot{m}_{in}$ is the inlet refrigerant mass flow rate, $h_{\lg} = h_g - h_l$ (h_l and h_g are refrigerant saturated liquid and vapor specific enthalpies).

In Eq. (2), the left hand side is the liquid mass change rate in the evaporator. On the right hand side, $q/h_{\lg}$ represents the rate of liquid evaporating into vapor, and $\dot{m}_{in}(1-x_0)$ is the inlet liquid mass flow rate.

The inlet refrigerant mass flow rate $\dot{m}_{in}$ is dependent on the expansion valve openning A_v, the low pressure P_e, and high pressure P_c and can be expressed by

$$\dot{m}_{in} = A_v{}^a g_v(P_e, P_c) \qquad (3)$$

where a and $g_v(P_e, P_c)$ can be identified for a given expansion valve. P_e and P_c can be measured by two pressure sensors. For the two-phase section, the pressure is an invariant function of the temperature. Therefore, the inlet refrigerant mass flow rate $\dot{m}_{in}$ can be expressed as

$$\dot{m}_{in} = A_v{}^a g_v(T_e, T_c) \qquad (4)$$

Let's consider the vapor mass balance in an evaporator. The inlet vapor mass flow rate is $\dot{m}_{in} x_o$, and the outlet vapor mass flow rate is $\dot{m}_{out}$ when superheat is present. The rate of vapor generated from liquid during the evaporation process in the two-phase section is $q/h_{\lg}$. The time rate change of vapor mass should be equal to the inlet vapor mass flow rate plus the rate of vapor generated from liquid minus the outlet vapor mass flow rate. Assuming that the vapor volume is much larger than the liquid volume in the low-pressure side, we can obtain the vapor mass balance equation in an evaporator.

$$\frac{dM_v}{dt} = V \frac{d\rho_g(T_e)}{dT_e}\frac{dT_e}{dt} = \dot{m}_{in} x_o + \frac{q}{h_{\lg}} - \dot{m}_{out} \qquad (5)$$

where M_v is the total vapor mass of the low-pressure side and V is the total volume of the low-pressure side, ρ_l is the saturated vapor density of refregirant in a function of evaporating temperature T_e. The outlet refrigerant mass flow rate is the same as the compressor mass flow rate, which is dependent on the compressor speed, the low pressure P_e and high pressure P_c. This mass flow rate can be expressed by

$$\dot{m}_{out} = \omega g(P_e, P_c) \qquad (6)$$

where $g(P_e, P_c)$ can be identified for a given compressor. As said before, the pressure is an invariant function of the temperature for the two-phase section. Therefore, the outlet refrigerant mass flow rate can be expressed as

$$\dot{m}_{out} = \omega g(T_e, T_c) \qquad (7)$$

Therefore, Eq. (5) can be written as

$$\frac{dT_e}{dt} = \frac{\pi D_i \alpha_i}{k h_{\lg}} l (T_w - T_e) + \frac{x_o}{k}\dot{m}_{in} - \frac{1}{k}\dot{m}_{out} \qquad (8)$$

where $k = V \frac{d\rho_g(T_e)}{dT_e}$.

Based on Eq. (1), (2) and (5), the state space representation for the low evaporator model is given below,

where T_e, l and T_w are the three states of the model, and T_a, $\dot{m}_{in}$ and $\dot{m}_{out}$ are the inputs to the system.

$$\begin{pmatrix} \dot{T}_e \\ \dot{T}_w \\ \dot{l} \end{pmatrix} = \begin{pmatrix} \frac{\pi D_i \alpha_i}{k h_{\lg}} l(T_w - T_e) + \frac{x_o}{k}\dot{m}_{in} - \frac{1}{k}\dot{m}_{out} \\ \frac{1}{(C_p \rho A)_e}(\pi D_o \alpha_o (T_a - T_w) - \pi D_i \alpha_i (T_w - T_e)) \\ \frac{1}{\rho_l (1-\bar{\gamma}) A}(-\frac{\pi D_i \alpha_i l (T_w - T_e)}{h_{\lg}} + \dot{m}_{in}(1 - x_o)) \end{pmatrix} \quad (9)$$

Eq. (9) shows that the evaporator dynamics are nonlinear. Specifically, the nonlineality comes from the bilinear function of l and T_w- T_e.

For the nonlinear feedback linearization control of HVAC systems [He and Asada, 2003], the heat transfer rate of evaporators must be estimated because no direct measurement or estimation is available. Based on the knowledge of T_e, l and T_w, the heat transfer rate q can be calculated using

$$q = \pi D_i \alpha_i l (T_w - T_e) \quad (10)$$

Because only T_e can be easily measured using a thermal couple, our task is to design an observer to estimate the value of the length of two-phase section l and the wall temperature T_w.

III. Nonlinear Observer Design for Evaporator

In this section, we will discuss nonlinear observer design for an evaporator to estimate the length of the two-phase section and the wall temperature T_w dynamically.

The following dynamics of the non-linear observer are proposed.

$$\begin{pmatrix} \dot{\hat{T}}_e \\ \dot{\hat{T}}_w \\ \dot{\hat{l}} \end{pmatrix} = \begin{pmatrix} \frac{\pi D_i \alpha_i}{k h_{\lg}} \hat{l}(\hat{T}_w - \hat{T}_e) + \frac{x_o}{k}\dot{m}_{in} - \frac{1}{k}\dot{m}_{out} \\ \frac{1}{(C_p \rho A)_e}(\pi D_o \alpha_o (T_a - \hat{T}_w) - \pi D_i \alpha_i (\hat{T}_w - \hat{T}_e)) \\ \frac{1}{\rho_l (1-\bar{\gamma}) A}(-\frac{\pi D_i \alpha_i \hat{l} (\hat{T}_w - \hat{T}_e)}{h_{\lg}} + \dot{m}_{in}(1 - x_o)) \end{pmatrix} - \begin{pmatrix} L_1 \\ L_2 \\ L_3 \end{pmatrix} (\hat{T}_e - T_e) \quad (11)$$

where $\hat{T}_e$, $\hat{l}$ and $\hat{T}_w$ are dynamic estimations based on the proposed observer, and T_e is the actual sensor measurement. L_1, L_2, and L_3 are the observer gains. The first part of the observer utilizes the nonlinear model for evaporator, and the second part is the feedback compensation based on the error between the measured evaporating temperature and the estimated value.

The question is how we can guarantee that the estimated state variables converge to the actual states of the plant. The contraction theory provides a straightforward procedure for assuring convergence [Lohmiller and Slotine, 1998]. According to the contraction theory, the system $\dot{\underline{x}} = f(\underline{x}, t)$ is said to be contracting if $\partial f / \partial x$ is uniformly negative definite. All system trajectories then converge exponentially to a single trajectory, with convergence rate $|\lambda_{\max}|$, where $\lambda_{\max}$ is the largest eigenvalue of the symmetric part of $\partial f / \partial x$. Therefore, if the actual states are particular solutions of the observer and the observer is contracting, then we can conclude that all the trajectories of the observer will converge to the actual states.

Fig.2 shows the evaporator dynamics and the observer structure.

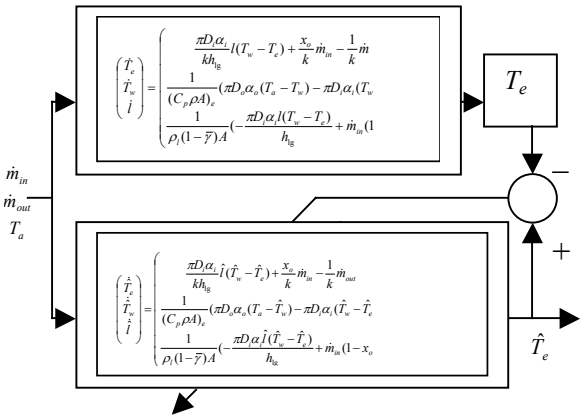

Fig. 2. Observer Structure

From the proposed observer dynamics, we can see that if $\hat{T}_e$ is equal to T_e, the observer dynamics are the same as the system dynamics. So the actual states that are the solutions of this set of equations are particular solutions of the observer. If the symmetric part of the Jacobian matrix of the observer dynamics is uniformly negative definite, then the trajectory of the observer dynamics will converge to the particular solution; this means the observed states are the same as the actual states.

The Jacobian matrix for the observer system is as follows

$$\frac{\partial f}{\partial x} = \begin{pmatrix} -\frac{B_3}{k h_{\lg}}\hat{l} - L_1 & \frac{B_3}{k h_{\lg}}\hat{l} & \frac{B_3}{k h_{\lg}}(\hat{T}_w - \hat{T}_e) \\ \frac{B_3}{B_1} - L_2 & -\frac{B_2 + B_3}{B_1} & 0 \\ \frac{B_3}{B_4 h_{\lg}}\hat{l} - L_3 & -\frac{B_3}{B_4 h_{\lg}}\hat{l} & -\frac{B_3}{B_4 h_{\lg}}(\hat{T}_w - \hat{T}_e) \end{pmatrix} \quad (12)$$

where

$B_1 = (C_p \rho A)_e$

$B_2 = \pi D_o \alpha_o$

$B_3 = \pi D_i \alpha_i$

$B_4 = \rho_l (1-\bar{\gamma}) A$

The symmetric part of the Jacobian matrix is as follow:

$$\frac{1}{2}\left(\frac{\partial f}{\partial x} + \left(\frac{\partial f}{\partial x}\right)^T\right) = \frac{1}{2}\begin{pmatrix} -2(\frac{B_3}{k h_{\lg}}\hat{l} + L_1) & \frac{B_3}{k h_{\lg}}\hat{l} + \frac{B_3}{B_1} - L_2 & \frac{B_3}{k h_{\lg}}(\hat{T}_w - \hat{T}_e) + \frac{B_3}{B_4 h_{\lg}}\hat{l} - L_3 \\ \frac{B_3}{k h_{\lg}}\hat{l} + \frac{B_3}{B_1} - L_2 & -\frac{2(B_2 + B_3)}{B_1} & -\frac{B_3}{B_4 h_{\lg}}\hat{l} \\ \frac{B_3}{k h_{\lg}}(\hat{T}_w - \hat{T}_e) + \frac{B_3}{B_4 h_{\lg}}\hat{l} - L_3 & -\frac{B_3}{B_4 h_{\lg}}\hat{l} & -\frac{2B_3}{B_4 h_{\lg}}(\hat{T}_w - \hat{T}_e) \end{pmatrix} \quad (13)$$

According to contraction theory, if the eigenvalues of this matrix are all negative, then the system is contracting. By looking at the characteristic equation $\lambda^3 + a_1\lambda^2 + a_2\lambda + a_3 = 0$, if $a_1 > 0$ and $a_1 a_2 - a_3 > 0$,

then the eigenvalues are all negative.

By choosing the appropriate values of L_1, L_2 and L_3, we computed the range of $\hat{l}$ and $\hat{T}_w - \hat{T}_e$ such that $a_1 > 0$ and $a_1 a_2 - a_3 > 0$ are satisfied as shown in Fig. 3.

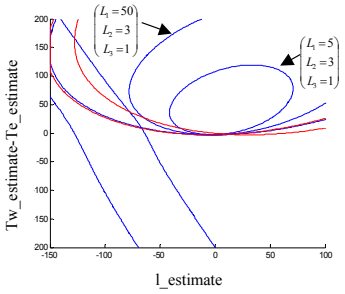

Fig.3. Convergence range for some sets of values of observer gains L_1, L_2, L_3

It is concluded that the sufficient condition for $a_1 > 0$ and $a_1 a_2 - a_3 > 0$ is L_1=200, L_2=30, L_3=1 by considering the operation space of $\hat{l}$ and $\hat{T}_w - \hat{T}_e$ as shown in Fig. 4 and Fig. 5.

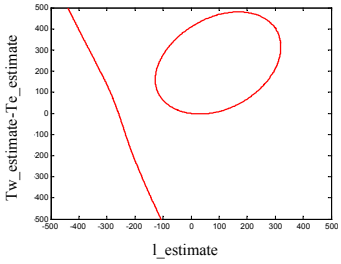

Fig.4. Convergence range for L_1=200,L_2=30,L_3=1

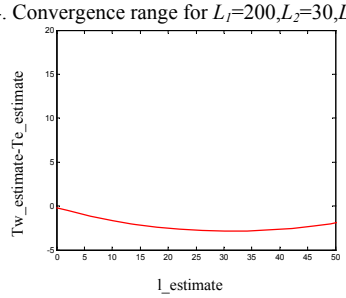

Fig.5. Zoom plot of the convergence range for L_1=200,L_2=30,L_3=1

Therefore, L_1=200, L_2=30 and L_3=1 is a sufficient set of gians to ensure that the Jacobian matrix of the observer model is negative definite. Based on contraction theory, the observer states will converge to the actual states of the evaporator model because the observer dynamics have been designed in such a way that the original states of the model are the particular solutions of the observer model.

IV. Simulation and Experimental Results

The observer design was evaluated by a matlab simulation. For comparison, a standard linear observer is used for the linearized model of the evaporator. Around some operation point, the linearized model of the evaporator is given by:

$$\begin{Bmatrix} \partial \dot{T}_e \\ \partial \dot{T}_w \\ \partial \dot{l} \end{Bmatrix} = \begin{pmatrix} -\frac{B_3}{kh_{lg}}\bar{l} & \frac{B_3}{kh_{lg}}\bar{l} & \frac{B_3}{kh_{lg}}(\bar{T}_w - \bar{T}_e) \\ \frac{B_3}{B_1} & -\frac{B_2+B_3}{B_1} & 0 \\ \frac{B_3}{B_4 h_{lg}}\bar{l} & -\frac{B_3}{B_4 h_{lg}}\bar{l} & -\frac{B_3}{B_4 h_{lg}}(\bar{T}_w - \bar{T}_e) \end{pmatrix} \begin{Bmatrix} \partial T_e \\ \partial T_w \\ \partial l \end{Bmatrix} + \begin{pmatrix} \frac{x_0}{k} & -\frac{1}{k} & 0 \\ 0 & 0 & \frac{B_2}{B_1} \\ \frac{(1-x_0)}{B_4} & 0 & 0 \end{pmatrix} \begin{Bmatrix} \partial \dot{m}_{in} \\ \partial \dot{m}_{out} \\ \partial T_a \end{Bmatrix} \quad (14)$$

The operation point used in the standard linear observer is chosen to be the same as the initial condition of the nonlinear observer. Fig. 6a,b and c show that the nonlinear observer states converge to the actual states of the system. However, the linear observer states do not converge to the actual states. This is because the standard linear observer for the linearized model can only guarantee the convergence of $\partial T_e, \partial T_w$ and ∂l but not T_e, T_w and l. The error has two sources. The first sourse is the linearization of the model, which is an approximation of the system at small vicinity around the operation point. The second source of error is the estimation of the operation point. The standard linear observer for the linearized model is not initial condition forgotten which makes the nonlinear observer necessary in this application.

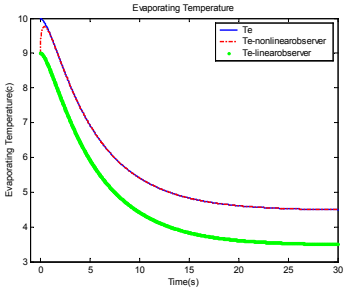

Fig.6a. Comparison of T_e

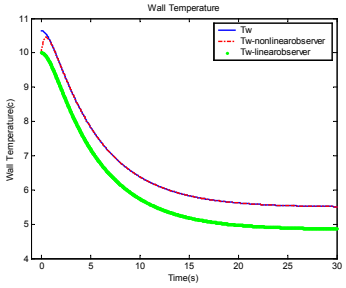

Fig.6b. Comparison of T_w

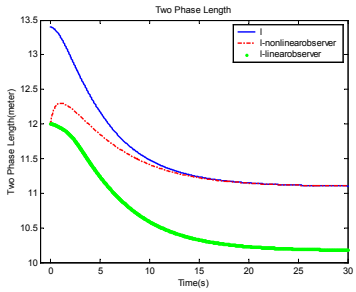

Fig. 6c. Comparison of l

With the three trajectories converging in the nonlinear observer, it is expected that the value of heat transfer rate q

also converge to the real value of q as shown in Fig. 6d.

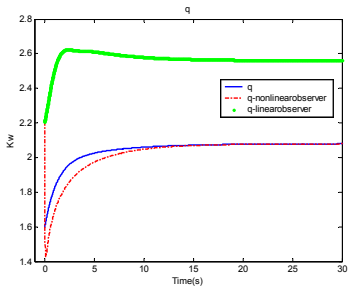

Fig.6d. Convergence of q

Experiments have been conducted to verify the evaporator observer design. The test equipment is a 2.8kW split type air conditioner for residential applications. The machine is equipped with variable speed compressor and electronic expansion valve. The initial operating conditions are listed: Outdoor temperature: 35C; Indoor temperature: 20C; Compressor Speed: 70Hz; Electronic Expansion valve: 15 Steps; Indoor fan speed:1250rpm; Outdoor fan sped: 630rpm

Then the outdoor temperature changed from 35C to 27C. The room temperature T_a and evaporating temperature T_e were measured. The observer design described in section 3 is used with the actual data from the measurement sensor. Fig. 7 shows the structure of the observer for the experiment.

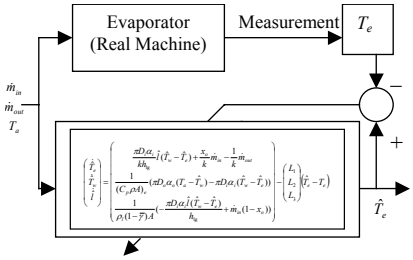

Fig.7. Observer structure with experiment data

Fig. 8 shows the comparison of the various determinations of the evaporating temperature T_e. The measured evaporating temperature T_e is from the temperature sensor. The simulated T_e is obtained from simulating the evaporator nonlinear dynamics Eq.(9) with the initial conditions set equal to the experimental data. The observed T_e ($\hat{T}_e$) is from the observer for the evaporator shown in Fig. 7. It can be seen that the estimates of T_e from the observer match very well with the experiment measurements. The results from the evaporator nonlinear dynamics simulator are also shown in Fig. 8. There is some discrepancy between the simulated results and the measured data. It results from the model error of the simulator. However, there is a feedback term in the observer structure as shown in Fig. 7 which can compensate for the model error. It can be seen that the estimated T_e from the observer is much closer to the experiment data than the simulated T_e from evaporator model. And from the contraction theory, initial conditions of the observer dynamics are forgotten. Although the observer starts with the different initial conditions, its states converge to the experimental data very quickly. Fig. 9 and Fig. 10 show the results for the wall temperature and two-phase length. The observed values are compared with the values from the evaporator model simulator because there are no measurements for these two variables. There are some discrepancies between the observed results and the simulated results. They may derive from the model error of the model simulator.

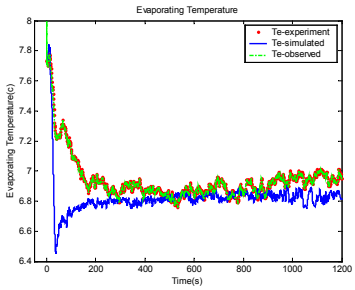

Fig.8. Comparison of the evaporating temperature

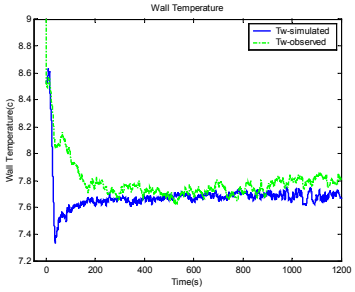

Fig.9. Comparison of the wall temperature

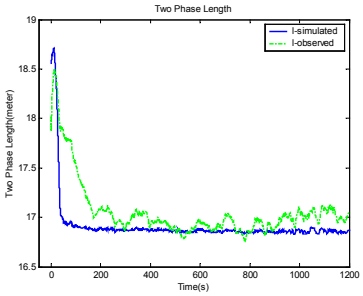

Fig.10. Comparison of the two-phase length

V. Feedback Linearization Control of Evaporating Temperature with the Model-Based Nonlinear Observer

Feedback linearization nonlinear control was recently proposed to control the evaporating temperature [He and Asada, 2003]. An estimate of heat transfer rate for evaporator is needed for feedback linearization compensation. With the nonlinear observer design discussed in Section 2, an integrated control scheme is

presented to combine the nonlinear controller and the observer. Fig. 11 shows the block diagram of the integration of the nonlinear controller and the observer.

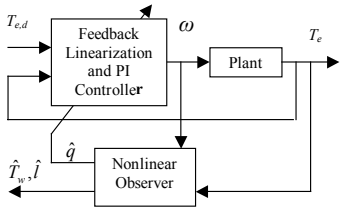

Fig.11. Block Diagram of the integration of the Nonlinear Controller and the Observer

Some simulation results are shown below. It is assumed that :Inlet vapor quality x_0 =0.2; Setpoint of evaporating temperature $T_{e,d} = 10^o C$; Initial evaporating temperature $T_e(t=0) = 14^o C$; Room air temperature $T_a = 27^o C$

The input of inlet mass flow rate is shown in Fig. 12.

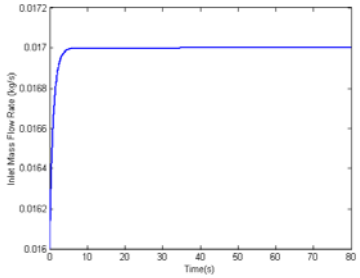

Fig.12. Input of the inlet mass flow rate

Fig. 13-14 show the comparison results between the conventional PI control and integrated nonlinear control/observer shown in Fig. 11. The same PI gains are used in both PI control and PI part of the nonlinear control. The simulation results plotted in Fig. 13 show that the performance of the nonlinear control is better than the conventional PI control.

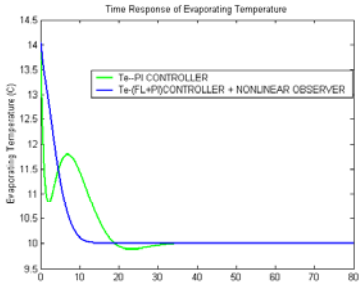

Fig.13.Comparison of the response of evaporating temperature

When the model-based nonlinear observer has some parameter error, the PI control part in the nonlinear control can compensate for it. Fig. 14 shows that the control performance of the nonlinear control is still better than the conventional PI control despite these parameter errors.

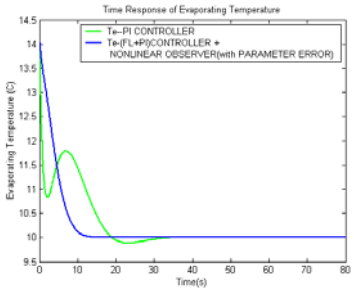

Fig.14. Comparison of the response of evaporating temperature

VI. CONCLUSIONS

The model-based nonlinear observer design presented in this paper can estimate dynamic variables of the evaporator with guaranteed convergence. This is demonstrated with simulation and experimental results. Feedback linearization with a PI controller and a model-based nonlinear observer can achieve the desired performance of the evaporating temperature control. This observer design for the evaporator will also be used for the investigation of dynamic refrigerant distribution model in the future.

REFERENCES

[1] Chi, J., and Didion, D., 1982, "A simulation of the transient performance of a heat pump", *Int. J. Refrigeration*, Vol. 5, No. 3, pp. 176-184.

[2] Harms, T., Groll, E., and Braun, J., 2003, "Accurate Charge Inventory Modeling for Unitary Air Conditioners", *International Journal of HVAC & R Research*, Vol. 9, No. 1, pp. 55-78

[3] He, X., Liu, S., and Asada, H., 1997, "Modeling of vapor compression cycles for multivariable feedback control of HVAC systems", *ASME Journal of Dynamic Systems, Measurement, and Control*, Vol. 119, pp. 183-191.

[4] He, X., and Asada, H., 2003, "A New Feedback Linearization Approach to Advanced Control of Multi-Unit HVAC Systems", *Proceedings of the American Control Conference*, Denver, Colorado, June, 2003, pp.2311-2316.B. Smith, "An approach to graphs of linear forms (Unpublished work style)," unpublished.

[5] Lohmiller, W., and Slotine, J-J, 1998, "On Contraction Analysis for Non-linear Systems", *Automatica,* Vol.34, No.6, pp.683-696.

[6] MacArthur, J. W., and Grald, E. W., 1989, "Unsteady compressible two-phase flow model for predicting cyclic heat pump performance and a comparison with experimental data", *Int. J. Refrigeration*, Vol. 12, pp. 29-41.

[7] Slotine, J-J and Li, W., 1991, *Applied Nonlinear Control,* Prentice Hall, New Jersey

[8] Wedekind,G.L.,Bhatt,B.L., and Beck, B.T., 1978, "A system mean void fraction model for predicting various transient phenomena associated with two-phase evaporating and condensing flows," *Int. J. Multiphase Flow*, Vol. 4, pp. 97-114.